Republic of Bulgaria
Sofia University "St. Kliment Ohridski"
Faculty of Physics
Department of Optics and Spectroscopy

Extrapolation properties of the Morse-Long Range potential at large internuclear distances

Ph. D. Thesis
of
ALKETA SINANAJ

Scientific Supervisor:

Prof. DSc. Asen Pashov

Sofia, 2024

Contents

Chapter 1 Introduction

The potential energy curve is among the main concepts in molecular physics and particularly for diatomic molecules. It is very difficult even to mention all studies which rely on some knowledge of the potential functions. Relatively recently, however, the need for accurate potential energy curves (PEC) appeared. In our opinion, it is not the spectroscopic community who gradually realized the advantages which the potentials offer compared to the more traditional molecular constants. It is just the emergence of easily available powerful computers in the late 90's of the 20^{th} century. Before that time, theoretical potential curves were calculated on big machines, but their use was limited to calculation of Frank-Condon and some basic molecular properties, because their accuracy was not sufficient to model the experimental spectra.

Some methodology for solving the inverse problem, i.e. spectra $\rightarrow$ potential was developed already in 1930's by Rydberg, Klein and Rees [1], [2]. Although semiclassical, this procedure was the only one widely used by spectroscopists until 1990's because it was simple to use but also quite accurate compared to the *ab initio* curves. Another, fully quantum mechanical procedure appeared in 1970's by W. Kosman and J. Hinze and C. Vidal and H. Scheingraber [3], [4]. Unfortunately, the ideas in these early papers were not successfully realized, although some attempts have been made.

In the late 1990's several groups realized that the power of personal computers became sufficient to solve some of the inverse problems. Moreover, since these computers were already widely spread it was possible to distribute the derived empirical potentials and also computer codes within the community, so that the potential curves may become a standard tool for modeling molecular spectra, like the molecular constants until then. Among the advantages of the potential curve approach over the one with molecular constants one should mention:

- Possibility to calculate both energies of levels and intensities of spectral lines.
- PECs have known asymptotic behavior and therefore better extrapolation properties. Empirical curves may be compared and/or extended by ab initio calculations.
- PECs are applicable to electronic states with irregular shapes, very different from Morse potential.
- More consistent approach to model perturbations in spectra because various matrix elements may easily be calculated.
- PECs are directly applicable in scattering calculations.

This advance in molecular spectroscopy coincided with the rapid development of laser colling and trapping of atoms (Nobel Prize in Physics, 1997). Understanding the interactions between cold atoms at very low temperatures became extremely important, thus the need for accurate potential curves close to the corresponding atomic asymptotes. Many approaches, based

on the purely long-range dispersion form of the potential have been developed (for example [5], [6] and references therein).

The long-range part of the potentials has been extensively studied also by spectroscopists. Already in 1970's LeRoy and Bernstein [7] proposed a formula with molecular constants suitable to fit the near asymptotic levels of a diatomic molecule – the so called Near-Dissociation-Expansion (NDE) ((2.74)- in the Thesis). Some of these constants were related to the long-range coefficients (C_3, C_6 etc.) so this formalism builds a bridge between the spectroscopic observations (line frequencies, level energies) and the dispersion coefficients, which determine the interaction between the atoms at large internuclear distances.

The long-range part of the potential may be approximated with various mathematical expressions. They will be discussed later in the thesis. The most important part comes from the interaction of the various induced multipole moments:

$$U_{LR}(R) = D_e - \sum_n \frac{C_n}{R^n} \tag{1.1}$$

and it is, perhaps, the only part of the molecular potential for which a realistic expression may be derived. At smaller *R* other interactions contribute to the potential which depend on the electron configuration of the atoms and all associated interactions: Coulomb, spin-orbit, spin-spin and others. No physical models are available in this region, except for that near the minimum, the potential may be approximated with a parabola and on this approximation the concept of equilibrium molecular constants is based.

Within the thesis several analytic functions are presented, frequently used to model the shape of regular, Morse-like potentials. In some of them the function asymptotically approaches the long-range formula as $R \to \infty$. In another, the short-range potential function is truncated at some intermediate *R* and then the long-range part is attached in a continuous manner. Both approaches are discussed within the thesis. The question is how reliably one can determine the long-range part of the potential from limited sets of experimental data, which we usually have at our disposition. The importance of this question cannot be underestimated because the derived potential curves are used not only to model and to reproduce the experimental data. Often the potential can be used in other groups to calculate photoassociation rates, scattering lengths, Feschbach resonances and so on. They need to know how reliable the fitted potential is. Unfortunately, often the derived potentials are published as they are and no reliable estimates on their accuracy are available. At the same time, such estimates are not trivial at all. The connection between the potential function and the experimental energies is complex and the error-propagation analysis is not trivial. The fit is highly non-linear since the experimental observations are modelled not directly by the fitted function, but through the solutions of the radial Schrödinger equation, where the potential function is inserted. However, the Schrödinger equation itself is an approximation and the accuracy of the modern spectroscopy is high enough to detect various deviations from this approximation. In some

cases, the deviations may be accounted for effectively, in other cases – the approximation of the single Schrödinger equation fails, and the observations should be modelled via coupled channels calculations. So, building a physically consistent model is already a challenge which requires sufficient experience.

Once the model is adopted, error analysis may be carried out. Here problems are two. First, whether to use the matrix of variances and covariances, as in the usual linear fits, or to arrange a more sophisticated (and more time consuming) techniques like Monte-Carlo. The second, and a more general problem, do we estimate the uncertainty of the potential curve (or its dissociation energy, or the C_6 coefficient) or we estimate the uncertainty within the adopted functional form. For example, we may fit experimental data with a Morse function and then we may determine the uncertainty of the dissociation energy D_e. This uncertainty, however, is associated with the Morse function (and the experimental data) and does not come ONLY from the experimental data. This is the problem of model dependencies of the error estimates. In the ideal situation, we would like to report uncertainties which are (at least to a great extent) free from the choice of potential function. Having this in mind, we are going to determine the:

Goals of the thesis

Among the potential functions in the literature, we select the Morse/Long-Range model [8] which has a built-in long-range behavior and is discussed for having good extrapolation properties. We will examine these properties by fitting high quality experimental data on the ground state of Ca dimer. This state was studied experimentally already in 2002 [9] and 2003 [10]. Additionally high-quality estimates on the dispersion coefficients are available from different theoretical [11] and experimental sources [12], [13], [10]. The $^{40}Ca_2$ ground state has no hyperfine structure (nuclear spin for ^{40}Ca is I=0) and all excited states are well separated, so the single channel approach has already been shown to be very adequate.

(i) We need to develop methodology how to estimate the uncertainties of the main fitted long-range potential parameters: dissociation energy D_e and leading dispersion coefficient C_6 associated ONLY with the accuracy and the composition of the experimental data and NOT with the choice of MLR model.

If we manage to estimate the real uncertainties, then we may ask questions about the extrapolation properties of the MLR form.

(ii) How the uncertainties of D_e and C_6 can from the matrix of variances and covariances can be compared with the real uncertainties?

(iii) How accurately one can determine D_e and C_6 given a limited set of experimental data? The built in long-range form in MLR suggests that these estimates should be more accurate than by other potential forms.

Often experimental data can be combined with theoretical calculations to make better spectroscopic models. For example, the knowledge of C_8 and C_{10} from the theory, even to within 10-20 % uncertainty may help to improve the uncertainty of D_e and C_6 significantly.

(iv) So, we will study the uncertainties of D_e and C_6 depending on the composition of the long-range model (the number of long-range coefficients) and we will study to which extent the theoretical predictions may reduce the uncertainties.

Theory

Chapter 2 Energy levels of diatomic molecules

In this chapter the main concepts and the theory behind the energy levels structure of diatomic molecules are presented.

It is shown that by separating of radial and angular variables (similarly to the case of hydrogen atom) the problem of a diatomic molecule can be reduced to the radial Schrödinger equation:

$$\left[-\frac{\hbar^2}{2\mu}\frac{d^2}{dR^2}+\frac{\hbar^2}{2\mu R^2}(J(J+1)-\Omega^2)+U(R)\right]\Psi_{vJ}(R)=E_{vJ}\Psi_{vJ}(R) \qquad (2.1)$$

$J(J+1)-$ an eigenvalue of the square of the total angular momentum operator $\hat{J}^2$ $\Omega-$ projection of $\boldsymbol{J}$ on the internuclear axis, v and $J-$ vibrational and rotational quantum numbers. $U(R)$ is the potential energy curve which is the R dependent solution of the electron Schrödinger equation.

Inverted Perturbation approach (IPA)

IPA is a fully quantum mechanical method which optimizes a parametrized PEC in such a way that its eigen energies from the RSE agree with the experimental observations within their uncertainty. The method is accurate when a single channel RSE can model the experimental data.

From the experiment we have some set of energy levels $E_{vJ}^{experiment}$ and then we take an approximation for the PEC (*ab initio* or RKR), insert it in the Schrödinger equation and obtain $E_{vJ}^{calculate}$:

$$\left(\frac{\hbar^2}{2\mu}\frac{d^2}{dR^2}+U(R)+\frac{\hbar^2}{2\mu R^2}J(J+1)\right)\chi_{vJ}(R)=E_{vJ}^{calculate}\chi_{vJ}(R) \qquad (2.2)$$

We are searching for correction $\delta U(R)^{Correction}$ to the initial potential curve such that the calculated levels $E_{vJ}^{calculate}$ agree with $E_{vJ}^{experiment}$ in the Least-Squares-Approximation (LSA) sense:

$$U(R)^{True} = U_0^{Approximation} + \delta U(R)^{Correction} \tag{2.3}$$

If the correction is small, we can write that the shift of the energy levels due to the correction can be calculated by using the first order of perturbation theory:

$$\Delta E_{vJ} = < \chi_{vJ}^0 |\, \delta U(R) | \chi_{vJ}^0 > = \sum_i a_i < \chi_{vJ}^0 |\, \delta_i(R) | \chi_{vJ}^0 > \tag{2.4}$$

Therefore, knowing the approximate vibrational wave function from the Schrödinger equation we can calculate this correction. The correction can be written as a linear combination of some known basis function $\delta_i(R)$.

$$\delta U(R) = \sum_i a_i\, \delta_i(R) \tag{2.5}$$

These $\delta_i(R)$ are known function, and a_i are unknown coefficients.

So, we see that the correction for energy level due to the change of the potential curve can be written as a linear combination of some known quantities $< \chi_{vJ}^0 |\, \delta_i(R) | \chi_{vJ}^0 >$.

The experimental energy should be equal to the corrected energy levels so:

$$E_{vJ}^{experiment} = E_{vJ}^{0\ approx} + \Delta E_{vJ} = E_{vJ}^0 + \sum_i a_i < \chi_{vJ}^0 |\, \delta_i(R) | \chi_{vJ}^0 > \tag{2.6}$$

Finally, the problem is reduced to a solution of system of linear equations in LSA sense:

$$E_{vJ}^{expe} - E_{vJ}^{0\ approx} = \Delta E_{vJ} = \sum_i a_i\ K_{vJi} \leftrightarrow \vec{b} = \vec{A} \cdot \vec{a} \tag{2.7}$$

The solution $\vec{a}$ gives us a better approximation for the PEC $U^1(R) = U^0(R) + \sum_i a_i\, \delta_i(R)$ and the whole procedure may be repeated until a sufficient agreement with the experiments is reached.

Generally U(R) and $\delta U(R)$ can have arbitrary functional form, like in the original papers by Kosman and Hintze [3] and Vidal and Scheingraber [4]. However, then the question arises how to add them and to work with a single function.

If we have a flexible functional form which is able to represent the searched PEC, $U(R,\vec{a})$, it is possible to derive a simple expression for the correction $\delta U(R)$ by writing the Taylor series:

$$U(R,\vec{a}) \approx U(R,\vec{a}_0) + \sum_i \frac{\partial U(R)}{\partial \alpha_i}(a - a_i^0) \tag{2.8}$$

Here $U(R,\vec{a}_0)$ is the initial potential PEC and:

$$\delta U(R) = \sum_i \frac{U(R,\vec{a}_0)}{\partial a_i} \cdot \left(a_i - a_i^0\right) \tag{2.9}$$

Obviously $\delta_i(R) = \frac{U(R,\vec{a}_0)}{\partial a_i}$ and we search for the correction $\Delta\vec{a}_i = \vec{a}_i - \vec{a}_i^0$

Long range part of the PEC

It is suitable to divide the potential into three important parts short-range, intermediate-range and long-range. In the intermediate range, around the equilibrium distance, the covalent bond dominates. At short internuclear distances, nuclear repulsion is important, and it corresponds to the steep repulsive wall of the PEC. The long-range (LR) starts from a sufficiently large *R* and goes to infinity, where the atoms do not interact, and the electronic wave function is a product of the atomic wave functions. At smaller *R* the strict limit for the LR is difficult to define, but approximately it is the distance at which the atomic wave functions start to overlap significantly.

The interactions in the LR region are mainly due to various electric multipole moments which the atoms induce in each other through weak Coulomb interactions [14]. The most important are the dipole, quadrupole and the octupole moments.

Then, by using the second order perturbation theory one can show that the general form of the long-range potential is:

$$U_{LR}(R) = D_e - \sum_n \frac{C_n}{R^n} \tag{2.10}$$

where D_e is the energy of the atomic asymptote; C_n are the so-called dispersion coefficients (Long range coefficients); *R* is the internuclear distance. The type of the leading dispersion coefficient depends on the atomic state to which the molecule dissociates. A detailed information on the prevalent terms in the expansion may be found in [15].

The long-range coefficients are the subject of both theoretical calculations [16], [17], [18], [19] and experimental research [10], [20]. Their importance cannot be underestimated, because they are related to the only part of the molecular potentials for which an accurate analytic functional form (2.10) exists. Often the question arises where exactly the long-range part of the potential starts? Strict answer cannot be given, but R. J. LeRoy in [15] suggested a quantitative criterion to determine the value of internuclear distance to make valid the expansion (2.10). The long-range expansion is expected to be valid for atomic separation larger than the so-called LeRoy radius R_{LR}, given by:

$$R_{LR} = \left[\langle r^2 \rangle_A^{\frac{1}{2}} + \langle r^2 \rangle_B^{\frac{1}{2}} \right] \tag{2.11}$$

where $\langle r^2 \rangle^{\frac{1}{2}}$ is the square root of the mean value of the squared radius of the external electron of the atom.

Chapter 3 Experimental determination of PECs

Motivation

As already said the potential energy curve is a zero-approximation concept to model the energy levels of a diatomic molecule. In many cases, this approach is fairly accurate and allows to reproduce the experimental observations to within $0.01 - 0.001\,\mathrm{cm}^{-1}$, i.e. about $1\,ppm$. Moreover, the model can be readily extended by coupling several electronic states considering various perturbations and achieving similar and even better accuracy [21], [22], [23], [24].

This chapter of the thesis is devoted to various mathematical expressions used to express a PEC as a function of R and some model parameters $\{\alpha_i\}$, which need to be adjusted in such a way that the PEC reproduces the experimental observations E_{vJ}^{exp} within their uncertainty. The connection between α_i and E_{vJ}^{exp} is through the radial Schrödinger equations, so by default the fit is not a linear one and one needs to care about all possible problems, associated with the non-linear curve fitting.

General requirements to the empirical Potential curves

The **first** and obvious **requirement** to the mathematical expression for $U(R, a)$ is to be flexible enough and to be able to precisely approximate any realistic shape. In Figure 3. 1 one can see as example the adiabatic potential energy curves for the first ten $^1\Sigma^+$ electronic states of the KRb.

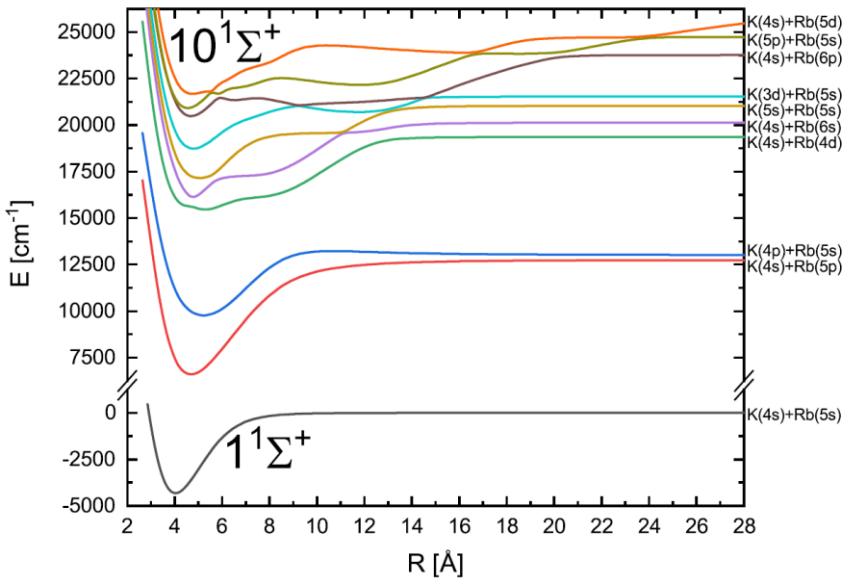

Figure 3. 1: Adiabatic potential energy curves for the (1–10) $^1\Sigma^+$ electronic states of the KRb molecule from [25].

Within this example one may see curves with "regular", Morse-like shapes, PEC with repulsive asymptote and a barrier (the (3)$^1\Sigma^+$ state), states with "shelf" region (the (5) and (6) $^1\Sigma^+$ state), double minima (the (7)$^1\Sigma^+$ state) and other even more complex shapes.

Obviously, too simple models like the Morse potential:

$$U_{Mo}(R) = D_e[1 - e^{-\beta(R-R_e)}]^2, \tag{3. 1}$$

parametrized with only 3 parameters, are too rigid to fit even the "regular" ground state potentials. On the other extremum are the infinite expansions over basis functions (preferably orthogonal) like the Dunham expansion of the PEC:

$$U(R) = \sum_{i=0}^{\infty} a_i \frac{(R - R_e)^i}{R_e} \tag{3. 2}$$

They are flexible, but also useless, because infinite summation is impractical.

The **second requirement** to the model PECs is to ensure the proper asymptotic behavior, namely:

$$U(R) \xrightarrow{R\to\infty} \text{const} \tag{3. 3}$$

$$U(R) \xrightarrow{R \to 0} \infty \qquad (3.\ 4)$$

The **third requirement**, although not strictly necessary, is that the potential curve should be smooth and differentiable. The radial Schrödinger equation may be solved also with non-smooth and not differentiable potentials. However, the nature of the problem, the Born-Oppenheimer approximation, which allows to separate the electrons motion from that of the nuclei, assumes slow variation of the electron energy over *R*. From a practical point of view, most of the numerical methods used for solving the RSE are much more effective and accurate if the PEC is smooth and differentiable.

R.J. LeRoy [8] also tries to provide some guidelines on the well-behaved forms to be used for potential energy curves. According to [8] function like this should satisfy the following criteria:

- It must be flexible enough to indicate very extensive, high-resolution data sets of experimental accuracy.
- It must be well-behaved, with no false extrapolation behavior outside the region where the experimental data are most sensitive.
- It must be smooth continuous everywhere and incorporate the correct theoretically known limiting behavior at large distances.
- It should be compact and portable and be defined by a relatively small number of parameters.

It is difficult to fulfil all these requirements in a single potential form. Actually, no such model has been proposed in the literature so far. The analytic models easily fulfil the third requirement, however it is difficult to combine flexibility and proper asymptotic behavior. Numerical, e. g. point-wise models are very flexible, but have no well-defined asymptotic behavior and are no differentiable. In the next section some of the successful models used in the literature are presented.

Analytic potentials

In this chapter of the thesis several analytic potential forms are presented in detail. These are:

- Morse potential
- Lenard-Jones potential
- Expanded Morse oscillator
- Morse-Lenard-Jones potential
- Morse/Long-range potential
- Chebyshev polynomials
- Hannover polynomials
- Spline point-wise form

In the Abstract, only the MLR form is discussed.

Morse-Long-Range

The Morse-Long-Range function is based on the MLJ (see Section 3.3.4 in the Thesis) by adding desired inverse power long-range behavior. The general form of MLR potential is [12], [8]:

$$V_{MLR}(r) = De\left(1 - \frac{U_{LR}(r)}{U_{LR}(r_e)} e^{-\beta(r)\cdot y_p^{eq}(r)}\right)^2 \tag{3. 5}$$

where

$$y_p^{eq}(r) = \frac{r^p - (r_e)^p}{r^p + (r_e)^p} \tag{3. 6}$$

$$y_p^{ref}(r) = \frac{r^p - (r_{ref})^p}{r^p + (r_{ref})^p} \tag{3. 7}$$

$$\beta(r) = \beta_{MLR}(r) = y_p^{ref}(r)\beta_\infty + [1 - y_p^{ref}(r)] \sum_{i=1}^{N} \beta_i [y_q^{ref}(r)]^i \tag{3. 8}$$

$$u_{LR}(r) = \frac{C_{m_1}}{r^{m_1}} + \frac{C_{m_2}}{r^{m_2}} + \cdots, \tag{3. 9}$$

and

$$\beta_\infty \equiv \lim_{r\to\infty}\{\beta(r)\cdot y_P^{eq}(r)\} = \lim_{r\to\infty}\{\beta(r)\} = \ln\left(\frac{2D_e}{u_{LR}(r_e)}\right) \qquad (3.\ 10)$$

The idea behind the variables $y_p^{eq}(r)$ and $y_p^{ref}(r)$ can be seen in Figure 3. 2.

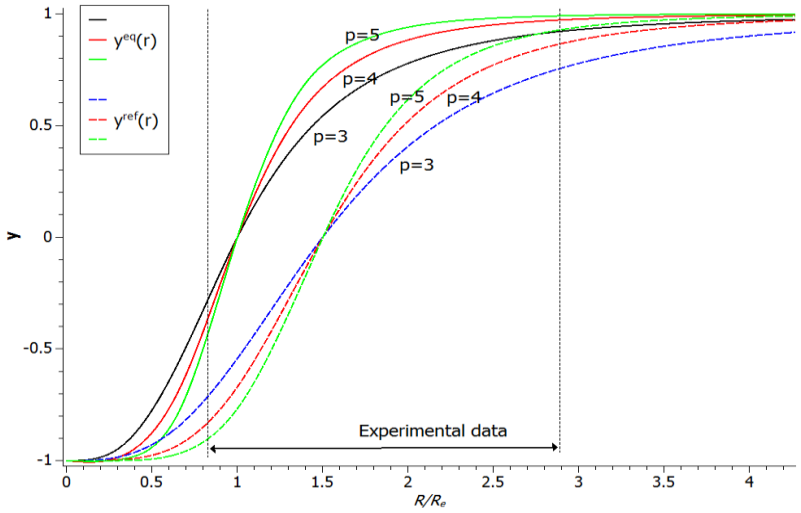

Figure 3. 2: Plot of the radial variables $y^{eq}(r)$ (solid curves) and $y^{ref}(r)$ (dashed curves) for various p.

The $y(r)$ variable has the nice feature, that at $r\to 0$ and $r\to\infty$ it reaches finite values of ±1, so the coefficients in the expansion will have finite values. The usual range of experimental data is also indicated. It may also be shown that at large r, the y variable becomes:

$$y_p^{eq} \xrightarrow{R\to\infty} 1 - 2\left(\frac{R_e}{R}\right)^p \qquad (3.\ 11)$$

Usually, r_{ref}, p, q and N are fixed, while β_i, D_e, C_m, r_e may be fitted to the experimental data. Around its minimum (r_e) the function retains its Morse-like character, since at $r = r_e$ $\frac{U_{LR}(r)}{U_{LR}(r_e)} = 1$. At large internuclear distances

$$V_{MLR}(r) \simeq \mathfrak{D}_e - u_{LR}(r) + \mathcal{O}\left(\frac{u_{LR}^2}{4\mathfrak{D}_e}\right) \qquad (3.\ 12)$$

And this makes the MLR function a very attractive one, combining both Morse-like behavior and proper long-range asymptote. The expression for $\beta(r)$ contains powers of *r* which can influence the asymptotic form (3. 12). Therefore, the power *p* must satisfy the condition [8]:

$$p > m_{last} - m_{first} \qquad (3.\ 13)$$

where m_{last} and m_{first} are the powers of the first and the last dispersion term in the long-range expansion. For example, $m_{first} = 6$ and $m_{last} = 10$, $p > 4$. There are no restrictions on the value of q, usually its value is smaller than p.

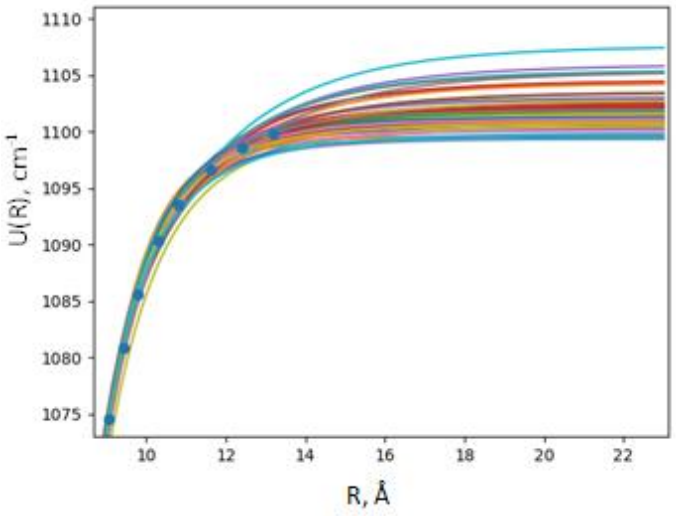

Re = 4.2778 +/- 0.0017
De = 1102.07 +/- 1.8
U_0 = 0.0 +/- 0.0
C6 = 11846306 +/- 7305389
C8 = 306079000 +/- 0.0
C10 = 8344000000 +/- 0.0
beta 0 = -1.1528 +/- 0.12
beta 1 = 0.0188+/- 0.5
beta 2 = -0.268 +/- 0.98
beta 3 = -0.191 +/- 1.6
beta 4 = -0.468 +/- 3.5
beta 5 = 0.247 +/- 3.1
beta 6 = -0.89 +/- 8.2
beta 7 = -1.20 +/- 6.8
beta 8 = 0.7 +/- 20.7
beta 9 = 1.9 +/- 17.8

Figure 3. 3: Fitting a MLR function with 10 parameters to empirical points of the Ca_2 X state [26] (solid circles). p=7, q=4 and $r_{ref} = 5.5$ Å. For more details, see the text.

In Figure 3. 3 we show a MLR function with *p=7*, *q=4* and $r_{ref} = 5.5$ Å. A Monte-Carlo simulation was performed as in (Section 3.3.3 in the Thesis) by adding synthetic noise to the empirical points (with a standard deviation of 1 cm^{-1}) and the resulted model parameters and their uncertainties were estimated. The fit virtually did not depend on C_8 and C_{10}, therefore their values remain unchanged. Strong correlations between the parameters exist. Their variation is significantly larger than the values themself.

If we reduce the number of coefficients to 4 (see Figure 3. 4), the fitted parameters are much more constrained. Here C_8 and C_{10} are fixed to zero without reducing significantly the quality of the fit. The value of D_e, however, is overestimated and the last three experimental points deviate significantly.

Apparently when using the MLR functional form one should be careful with the number of fitted parameters. The choice of fixed parameters (p, q, R_{ref}) should also be taken into account when studying the extrapolation properties.

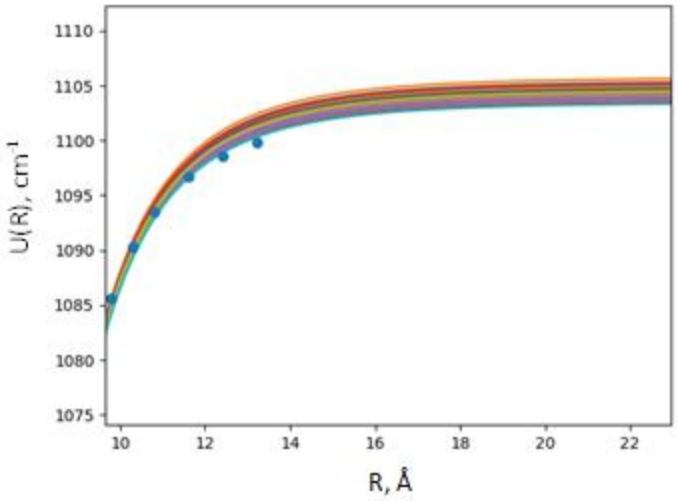

Re = 4.28092 +/- 0.00086
De = 1104.52 +/- 0.53
U_0 = 0.0 +/- 0.0
C6 = 17207259 +/- 424736
C8 = 0.0 +/- 0.0
C10 = 0.0 +/- 0.0
beta 0 = -0.3613 +/- 0.003
beta 1 = -0.2450 +/- 0.04
beta 2 = -0.297 +/- 0.09
beta 3 = 0.264 +/- 0.07

Figure 3. 4: Fitting an MLR function with 4 parameters to empirical points of the Ca_2 X state [26] (solid circles). p=7, q=4 and $r_{ref} = 5.5$ Å. For more details, see the text.

Comparison of the existing methods. Advantages and disadvantages

In this section most of the modern potential functions, used to model high resolution experimental observations, were presented. Depending on the application each of them has advantages and disadvantages and so far, no universal formula has been found. If one searches for a mathematically stable and flexible representation able to fit every, even an irregular shape – the spline point-wise functions have no competitors. All analytic potentials are smooth and differentiable, some of them offer proper asymptotic behavior.

One should keep in mind that the use of particular potential form may depend also on the quality and the composition of the experimental data. With abundant data sets, it is the data alone that fixes the shape of the potential and then, point-wise model-free functions are usually adequate. When the dataset is sparse, the empirical PEC is not uniquely defined, and the flexible point-wise potentials may show oscillations. Here analytic forms are of advantage.

The parameters of the point-wise potentials are local since they are the values of the potential function in the grid. The shape of the potential in every point depends only on the few nearby U_i parameters. This largely reduces the correlation between the potential parameters and makes the fits easier and more stable. In sparse data sets, this advantage turns into a problem, because the shape of the potential in regions badly described by the experimental data may become to a great extent arbitrary. The situation with the analytic potential is just the opposite. Due to correlations, the fitting process may be difficult, usually a good starting point is required. However, the shape of the fitted PEC is smooth. This property is of great advantage when extrapolating the potential shape in the asymptotic regions.

Chapter 4 Extrapolation properties of the MLR potential

In this chapter we present the main research on which the thesis is based. Given a set of experimental data we want to examine how reliably one can determine the depth of the potential well and the leading long-range term. Of course, it is assumed that the Born-Oppenheimer approximation is valid (in a broad sense) and that the single-potential approach is valid. In this sense, it is reasonable to choose an example without perturbations and no HF interaction at the asymptote.

As a testing case we chose the potential curve for the ground state of calcium dimer and the experimental data from [10]. The accuracy of this potential curve and especially its long-range part has been confirmed in a series of further studies – both from traditional spectroscopy and cold-collision experiments (see the Methodology of the Thesis).

In [10], Monte Carlo simulation was used to estimate the uncertainties of D_e, C_6 and C_8. Spline point-wise form was used for the inner part of the potential $U(r) = D_e - \frac{C_6}{r^6} - \frac{C_8}{r^8} - \cdots$ in the Thesis, and -for the outer. This approach offers a lot of flexibility, both sections of the potential are independent, and their shape is determined mainly through the experimental data. In the connection point the PECs are continuous but some of them are not necessarily smooth and in principle could be rejected. As already discussed, such an approach gives an upper estimate of the uncertainties.

The MLR form is entirely analytic. It is smooth and more rigid than the pointwise one. If its built-in long-range behavior provides better extrapolation properties, we should obtain a narrower spread of the fitted long-range parameters given the same experimental data. It is plausible to believe that the whole variety of MLR potentials will cover virtually all physical potentials consistent with the experimental data. However, if a rigid model is not the correct one, the narrower spread is by no means proof that the predictions are correct. So, it is important to check whether different constructions of the MLR potential fitted to different subsets of the same experimental data lead to similar long-range parameters, close to the "true" one. In [12], data from Allard et al. [10] were used to derive a series of MLR potentials and the recommended one by the authors has the same quality as the point-wise PEC, with very similar estimate on the long-range parameters. The uncertainties, however, are much smaller. They were deduced from the matrix of variances and covariances and they did not consider possible influence of the particular realization of the MLR potential (the so-called model dependencies). In Table 2 from Ref. [12] one can see that D_e and C_6 for different "good" potentials do not necessarily agree within the stated uncertainties. So,

the uncertainty of the fitted parameters alone cannot be used as a measure of how reliable the derived parameters are.

Given the abovementioned considerations we plan to conduct a comprehensive study of the MLR functional form and to check what are its extrapolation properties given a reasonably broad range of fixed parameters, which determine the function. If regardless of the particular choice of fixed parameters, we have a compact distribution of D_e and C_6 we will conclude that the extrapolation properties are good. In the opposite case, if the variation between D_e and C_6 is significantly larger than the uncertainty from a single fit, we will conclude that the MLR itself cannot confine the parameters and we shall search for additional considerations to limit the results from the fit. Such can be for example the expected ratio (from the theory) between C_6 and C_8 or similar.

Of course, the composition of the experimental data is crucial. It is unrealistic to expect experimental data with low v to lead to accurate value for D_e. It is natural to expect that the data should go beyond the LeRoy radius in order to expect somewhat reliable extrapolation. So, the above-mentioned studies should be conducted with different subsets of experimental data, gradually reducing the highest vibrational numbers.

Methodology of the study

Before explaining the details of the performed study, it is important to mention again briefly the goal and main ideas behind it.

The MLR potential form has a realistic built-in long-range behavior. It is plausible to expect that when applied to experimental data (even not covering the complete ranges of *v* and *J*) it will provide reasonably good estimates for the dissociation energy and the C_m coefficients. When speaking about the extrapolation properties of the MLR form it is necessary to consider not a single potential, but the whole class of curves defined by $\{r_{ref}, p, q, N, \beta_i, D_e, C_m, r_e\}$. So, it is important to study what is the influence of the prefixed parameters $\{r_{ref}, p, q, N\}$ on the fitted D_e and C_m.

There are two ways to estimate the uncertainty of the fitted parameters. The traditional one is through the matrix of variances and covariances [27]. It is strictly correct when the fit is linear. In non-linear cases (like the one we are dealing with), the matrix of variances and covariances provides a reasonable estimate only when the accuracy of the experimental data lead to very steep c^2 function and, as a consequence, the shape of c^2 may be reasonably well approximated with a paraboloid in the space of parameters (like in the linear case) within the estimated uncertainties of the fitted parameters. Even if the matrix of variances and covariances provides a reasonable estimate of the parameter uncertainties, it is an estimate for a given model $\{r_{ref}, p, q, N, \beta_i, D_e, C_m, r_e\}$. If one estimates the uncertainties from another model $\{r'_{ref}, p', q', N', \beta'_i, D'_e, C'_m, r'_e\}$ it is possible that the fitted D_e and $C_m$will not agree within their estimated uncertainties. These are the so-called model-dependences.

The second approach is not to rely on the quasi-linearity of the fit and to use a Monte Carlo simulation of synthetic experimental data (as done in [10] for the Ca_2 ground state). This approach, however, does not solve the problem with the model dependences of the estimated uncertainties.

In this study we used the matrix of variances and covariance to estimate the parameter uncertainties for every fitted PEC. Then we tried to repeat this procedure for a possibly large set of prefixed parameters $\{r_{ref}, p, q, N\}$ and in this way we study the effect of model dependences. In some cases, we directly studied the shape of c^2 along one of the parameters (for example $c^2(C_6)$) for more realistic estimate of its uncertainty.

In **Error! Reference source not found.** the block diagram of the performed series of fits is shown.

Initially we took the point-wise potential from [10], in a rather narrow range of $r \in [3.1, 10.8]$ Å and fitted various initial MLR potentials using the **betafit** code from [28], using different combinations of 4.3 Å $\leq r_{ref} \leq$ 6.7Å, $p \in [4, 9], q \in [3, 5], N \in [8, 11]$ (a total of nearly 300 combinations).

All these initial curves were further refined through a IPA8 code by fitting parameters β_i,

D_e, C_m, r_e until the fitted PECs reproduced all the 3586 experimental frequencies (with $v'' \leq 38$) as close to their uncertainties as possible. As a measure of the quality of the fit we used the dimensionless standard deviation σ:

$$\sigma = \sqrt{\frac{1}{(n-m)} \sum_{i=1}^{n} \frac{(E_{vJ}^{exp} - E_{vJ}^{calc})^2}{\sigma_{vJ}^2}} \tag{4.1}$$

The fitted potential was considered as good, if σ is about 0.62 – 0.64, comparable to the value from previous studies (see [10], [12]). All these fits were performed by using the Python shell to make the fitting faster.

These preliminary fits indicate that the correlations between D_e, C_6 and other parameters in the MLR form are strong. To reduce the uncertainties of D_e and C_6 we performed two additional series of fits by fixing C_{10} only and C_8 and C_{10}.

In a similar manner the simulation was repeated for three reduced data sets, namely with $v'' \leq 25, 30, 35$. When using point-wise potential with long-range extension [10] it was shown that the uncertainty of D_e and C_6 strongly depends on the presence of weakly bound energy levels. Increase of $v"_{max}$ from 35 to 38, reduced the uncertainties significantly.

As a result of this first stage of this study we derived 4 groups of potentials (for each data set) and each group contains 3 subsets – one with all C_m fitted, one with C_6 and C_8 fitted and one with only C_6 fitted. For each of these PECs the fitted parameters and their uncertainties from the matrix of variances and covariances were collected.

At the second stage, we examined to which extent the uncertainties derived in the first stage are reliable. We plotted a one-dimensional projection of $c^2(C_6)$ and compared this with the uncertainty from the matrix of variances and covariances. This step was much more time-consuming. For every class of potentials (defined by r_{ref}, p, q, N) we started to vary C_6 with small steps each time refining the potential in 10 – 20 iterations. The variation of C_6 was stopped when σ could not be reduced below 1. This second stage was performed automatically by the computer and as a result we collected several thousand possible combinations of long-range parameters. The step took 15 – 25 hours of computing time for an up-to-date personal computer.

To enable the automatized fitting, the selection of non-zero singular values was repeated after every iteration accounting for the change of σ. Without the automatic procedure such numerical experiments with thousands of fitted PECs are not possible. We are aware that it is very difficult to develop a perfect algorithm for unsupervised fitting. Therefore, it is not excluded that some of the "bad quality" fits could have been improved by more careful man-assisted fitting approach. We hope that such cases are few and they will not alter the overall results of the present study. During the first stage, when the different (r_{ref}, p, q, N) curves were fitted manually we got

impression on how stable and straightforward the fitting process is given reasonable initial values of the parameters. Based on this experience we chose the steps for changing C_6 in the second stage of the analysis such that the fit could converge in a reasonably small number of iterations. Usually, C_6 was changed in steps of 0.1% (for $v_{max} = 38$) and 1% (for $v_{max} = 25$).

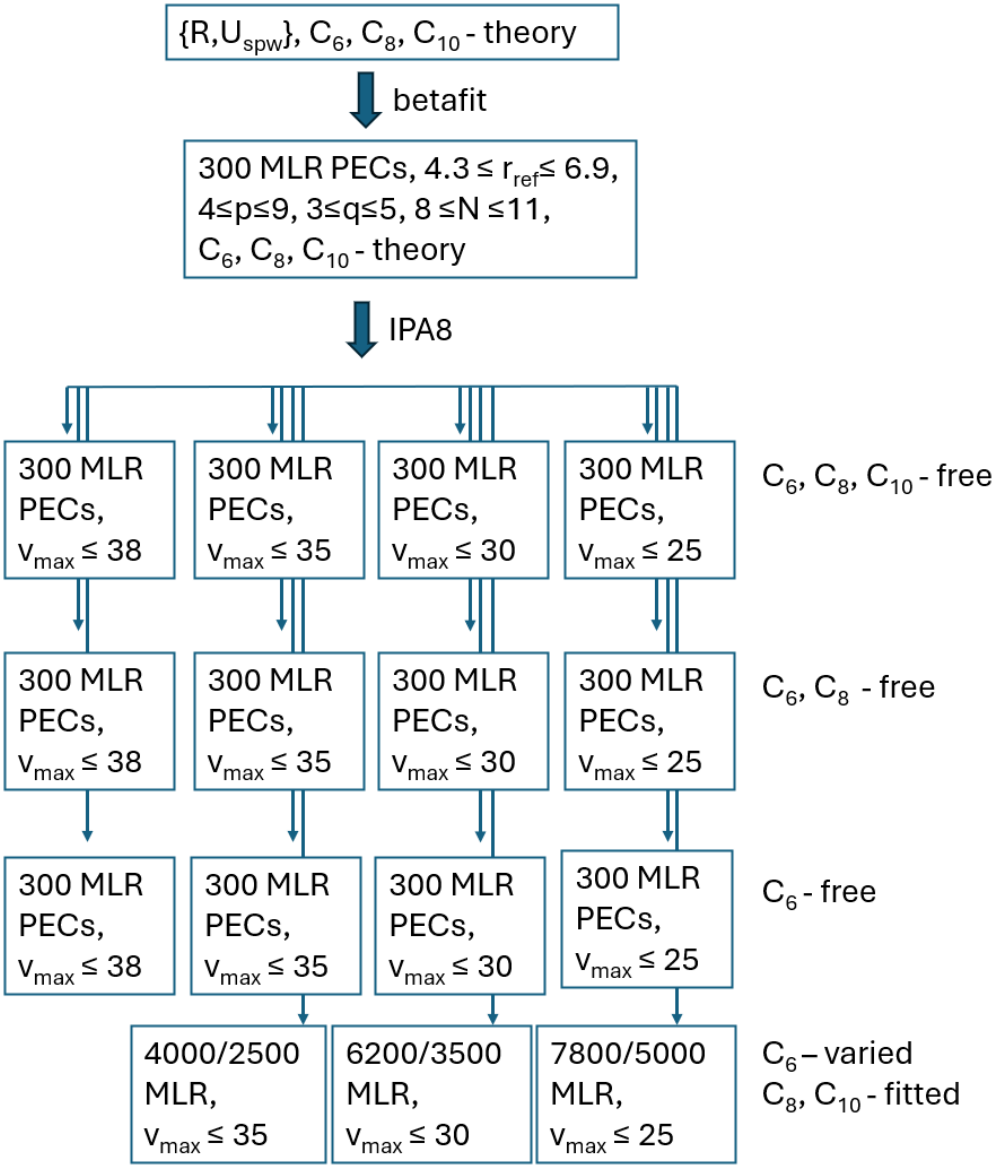

Figure 4. 1: Block-diagram of the fitting procedure.

When using point-wise potential with long-range extension [10], it was shown that the uncertainties of D_e and C_6 strongly depend on the presence of weakly bound energy levels. Increase of v″ max from 35 to 38, reduced the uncertainties significantly. If the extrapolation properties of the MLR potential are good, one can expect to see small variations of D_e and C_6 even for lower values of $v"_{max}$. How could this happen if the turning points for highest data points are

below the Le Roy radius? We think that due to the graduate transition between MLR and the long-range asymptote, it is rather the short-range shape of MLR, which is forced to have a proper behavior within the transition region. So, when fitting data with $v"_{max} = 25\ or\ 30$ it is mostly the β_i coefficients which are really fitted and the C_m/r^m plays effectively the role of regularization, which limits the unphysical behavior of the MLR potential at intermediate r (contrary to the MLJ potential, which may have an undesired maximum just beyond the range of experimental data [29].

During this study we tried to fit the experimental data also with MLR models with only one long range coefficient, C_6 (not shown in Figure 4. 1), and this turns out to be possible with very similar fit quality. In the next section we will compare the values we have obtained, but the conclusion is that C_8 and C_{10} cannot be determined from the present dataset. If added as parameters, they influence the fitted C_6 coefficient, but their values may be fixed within a very broad range without changing the quality of the fit. As demonstrated in the next section, the uncertainty of C_6 changes significantly depending on whether C_8 and C_{10} were hold fixed or fitted.

Chapter 5 Results

In this chapter the results from the fits, described in the previous chapter are presented. For each of the data sets from (**Error! Reference source not found.** in the Thesis) only potentials with $\sigma \leq 0.64$ are selected. The potentials were fitted having all parameters, including C_m coefficients, as free parameters. However effectively not always all combinations of parameters were fitted due to the SVD method. We gradually increased the number of non-zero singular values (thus including more and more parameters) until all parameters are treated as free or we reach values where the fit becomes unstable. As a result, often the values for C_{10} remain virtually unchanged and C_8 changed very little. When the standard errors of the fitted parameters were estimated we did not edit the singular values and let the matrix of variances and covariances to be calculated from the inverse of the design matrix as it is. In some cases, just for estimation of the uncertainties, we fixed C_8 and/or C_{10} and this, as expected, led to smaller standard errors of D_e and C_6.

Results for the full data set ($v \leq 38$)

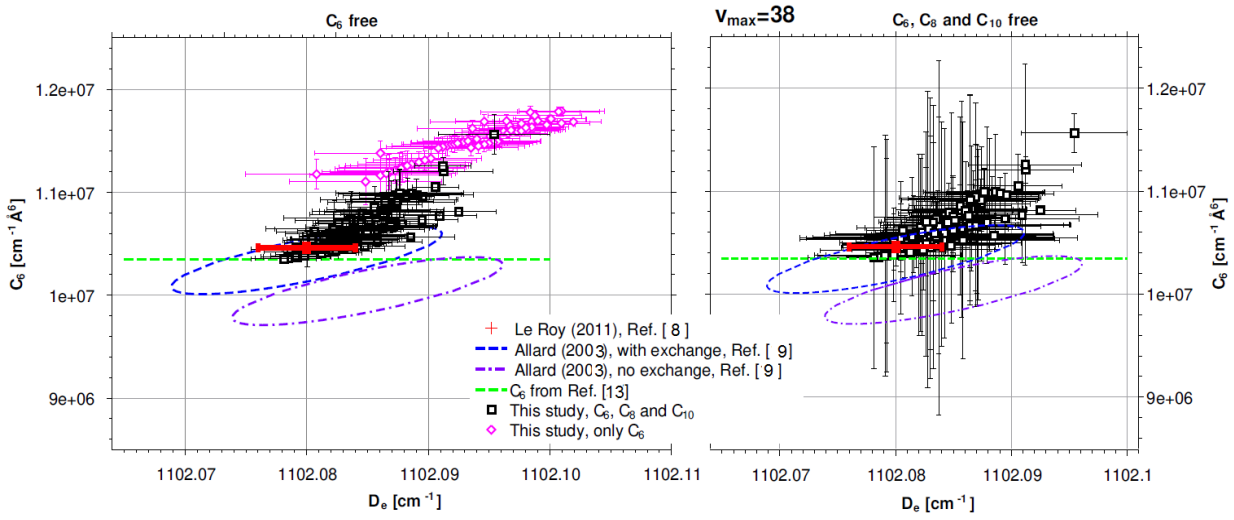

Figure 5. 1: Distribution of C_6 and D_e for MLR potentials (with $\sigma \leq 0.64$) with C_6, C_8 and C_{10} parameters fitted up to $v"_{max} = 38$ (open black squares). With open magenta diamonds we show the same distribution for MLR potentials with just one LR parameter, C_6. The The error bars are calculated with C_8 and C_{10} hold as fixed. (right pane) distribution of C_6 and D_e with the three LR coefficients, none of them fixed for calculating the uncertainties. For comparison with dashed ellipses the uncertainty limit from [10] is shown. The value from Ref. [8] is also shown with its uncertainty (red cross).

Figure 5. 1 shows the distribution of possible C_6 and D_e (open black squares) from fits including all experimental data ($v"_{max} = 38$). Error bars indicate the calculated σ standard deviation from the fit. For comparison the recommended values of $C_6 = (1.046 \pm 0.003) \times 10^7 cm^{-1}$Å^6 and $D_e = 1102.080 \pm 0.004\ cm^{-1}$ from the latest study [8] obtained when fitting

MLR forms to the same data set (with $v''_{max} = 38$) as here are added. The estimated uncertainties from [8] (also shown in Figure 5. 1 as a red point with error bars) are smaller than the region obtained in this study, and this demonstrates the influence of the choice of the fixed MLR model parameters. Under "region" we mean the area covered by the fitted points and their uncertainties.

In the left pane the uncertainties of C_6 and D_e from this study are estimated, as in Ref. [8], when C_8 and C_{10} are hold fixed. If they are treated as free parameters, the uncertainties in C_6 and D_e increase significantly – see the right pane. In the same Figure 5. 1 we added the estimated σ confidence regions from [10]. In this paper two values for C_6 were reported. One, $C_6 = (1.003 \pm 0.033) \times 10^7 cm^{-1}\text{Å}^6$ (lower ellipse in Figure 5. 1), obtained with simple long-range expansion ($U(r) = D_e - \frac{C_6}{r^6} - \frac{C_8}{r^8} - \cdots$) and another one $C_6 = (1.034 \pm 0.033) \times 10^7 cm^{-1}\text{Å}^6$ (upper ellipse), when the long range model was extended by expression for the exchange energy.

To underline the importance of the choice of the model, we also show the results from the present study when the MLR model was fitted with only one long range parameter – (open magenta diamonds). All four distributions are of similar size but shifted with respect to each other. At very long internuclear distances all models approach the same asymptotic form, $D_e - {C_6}/{r^6}$, but the ways how the potential transforms for intermediate r's is different and it is this region where D_e and C_6 are coupled to the rest of the potential parameters to ensure smooth transition.

After [10] several experimental papers addressed improved values for the Ca ground state C_6 coefficient. The most recent value can be found in the paper by E. Pachomow et al. [13], where results of two-colored photoassociation spectroscopy were reported. Some new bound vibrational states with $v'' = 38 - 40$ were observed, and their unperturbed energies were determined with very high accuracy ($E_{40} = 1.601(1)\ MHz$ and this may be compared with the prediction of the same energy from [10] $E_{40} \in [0.1, 2]\ MHz$). The long-range shape of the X state potential was reanalyzed, no exchange contribution was found to be necessary, but a retardation correction [11] to the C_6 term was applied. The recommended value for C_6 is $1.0348\ cm^{-1}\text{Å}^6$ (the excellent agreement with the second value from [10] should be a coincidence), but the authors write that no error limits are given for the individual long-range parameters from this work because of significant correlation between these parameters (caption of their Table II). It is outside the scope of the present thesis to study the statistical weight of different components of the long-range model from [13]. We will not focus on tiny differences of the C_6 coefficients fitted from spectroscopic data, but rather on the overall extrapolation properties of the MLR potentials, especially based on limited data sets.

The main result from these simulations ($v"_{max} = 38$) is that although the models can reproduce the experimental observations well the values of the fitted parameters may differ from model to model due to the interparameter correlations. For the moment we would conclude that with a limited data set it is not possible to fix in a unique way C_6 and D_e since their values will depend on whether other C_m coefficients, exchange energy or retardation effects are accounted for.

The model dependencies in the present case of Ca_2 are stronger than the uncertainties due to the experimental data.

Results for $v \leq 35$

In Figure 5. 2 we show the obtained distribution of D_e and C_6 for $v"_{max} = 35$. After the end of the fitting routine, the uncertainties of D_e and C_6 were calculated for two cases: both C_8 and C_{10} were treated as fixed parameters (upper pane) and only C_{10} fixed (lower pane). The correlation between C_8 and C_6 can be clearly traced by the significant increase of C_6 uncertainty when C_8 is also fitted.

On can see that by excluding the last three experimental vibrational levels the variation of D_e increases to about $\pm$ 0.1 cm^{-1} (C_8 and C_{10} fixed), almost an order of magnitude larger compared to the $v"_{max} = 38$ case. Similar estimate, Fig. 5 in [10], where the spline point-wise model extended with ($U(r) = D_e - \frac{C_6}{r^6} - \frac{C_8}{r^8} - \cdots$) is shown in Figure 5. 2 with an ellipse (blue dashed line). It should be compared with the more flexible estimations when C_6 and C_8 fitted, lower pane. The estimate of the uncertainty of the fitted parameters through the matrix of variations and covariations for the MLR potentials (black squares) is comparable to that in [10]. Since the uncertainties of C_6 at least for some potential forms are of the order of its value one may doubt if the estimation through the matrix of variances and covariances is still valid.

This can be checked by finding all MLR potentials which agree with the experimental data. Starting from about 300 different MLR potentials we varied C_6 until σ could not be reduced below 1. Altogether about 4000 PEC were fitted, of them 2500 with $\sigma \leq 0.64$. This second stage was performed automatically by the computer, and it took 15 – 25 hours of computing time for an up-to-date personal computer. Fitted D_e and C_6 are shown in Figure 5. 3. By comparing this figure with Figure 5. 2 we see that while the estimate for the D_e uncertainty by the variances turns out to be quite reasonable, the real variation of C_6 is significantly smaller. The uncertainty region from the MLR fit is still smaller than that from the pointwise one [10].

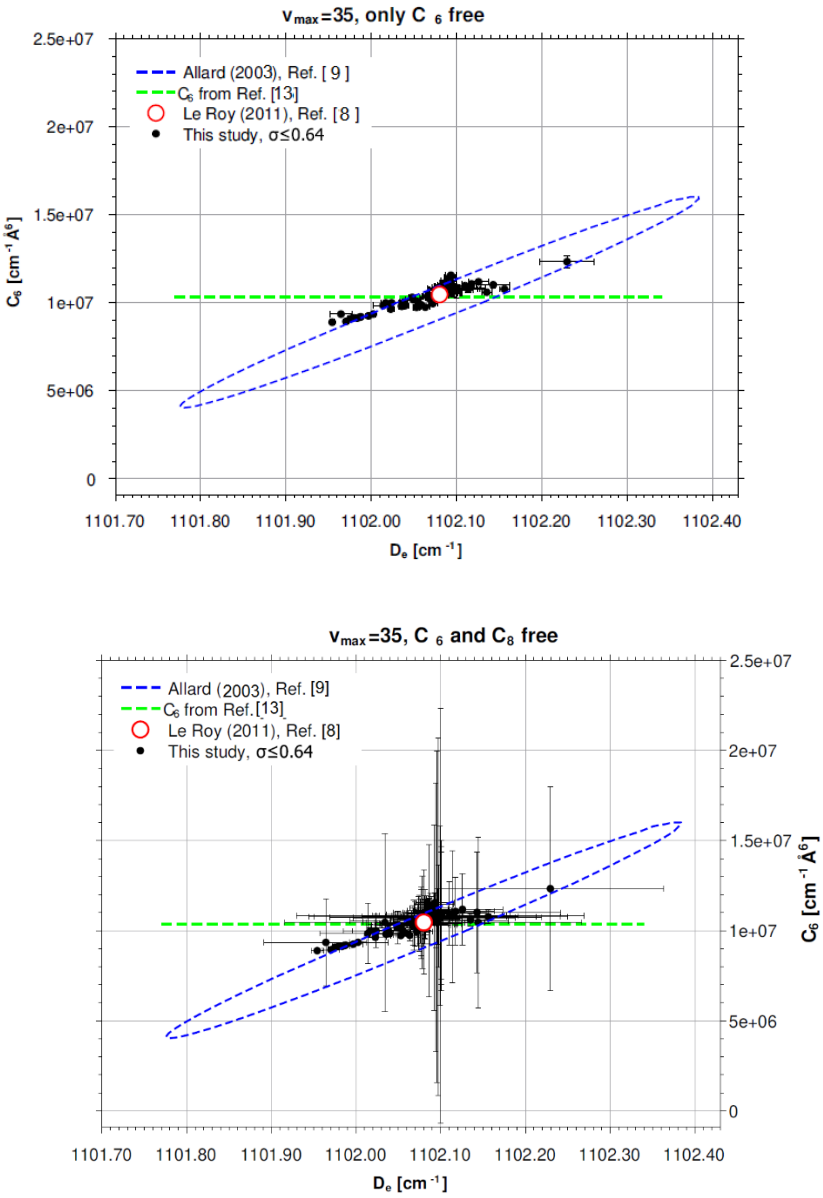

Figure 5. 2: Distribution of C_6 and D_e for MLR potentials (with $\sigma \leq 0.64$) fitted up to $v"_{max} = 35$. For comparison with dashed ellipse the uncertainty limit from [10] is shown. The value from Ref. [8] is also shown. In the upper pane C_8 and C_{10} were fixed for calculation of the uncertainties, in the lower pane – only C_{10} was fixed.

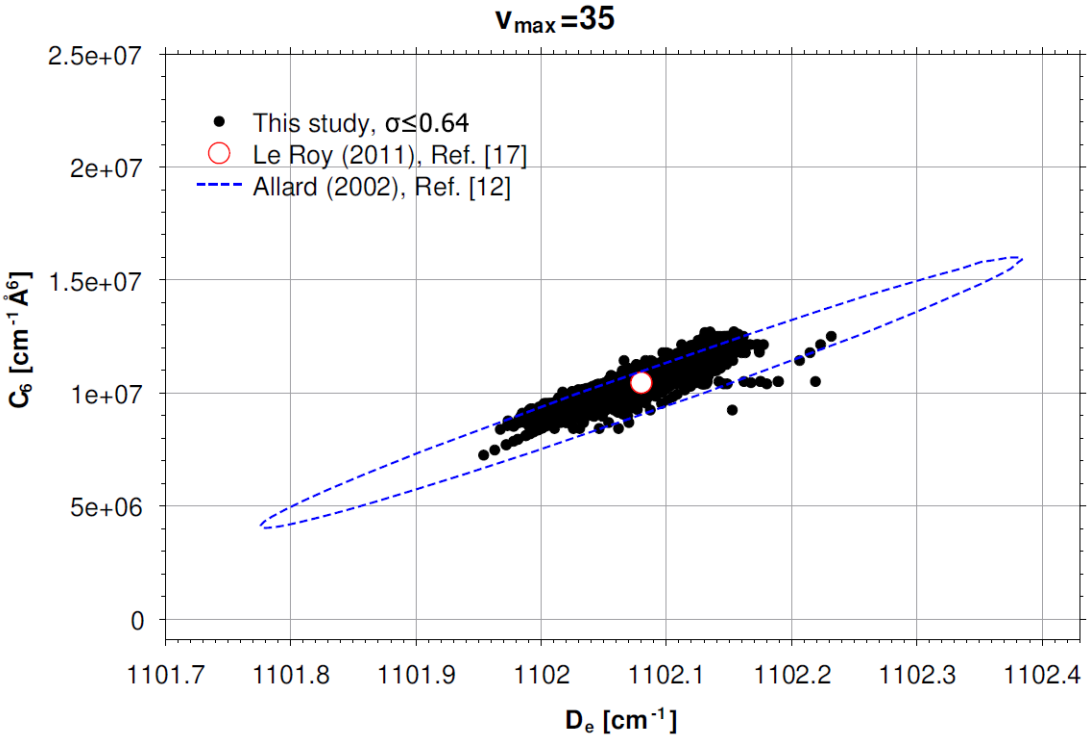

Figure 5. 3: Distribution of C_6 and D_e for MLR potentials (with $\sigma \leq 0.64$) fitted up to $v"_{max} = 35$ derived by fixing C_6 within a broad range of values and refitting all other parameters. With dashed ellipse the uncertainty limit from [10] are shown. The value from Ref [8] is also shown.

Results for v ≤30 and v ≤25

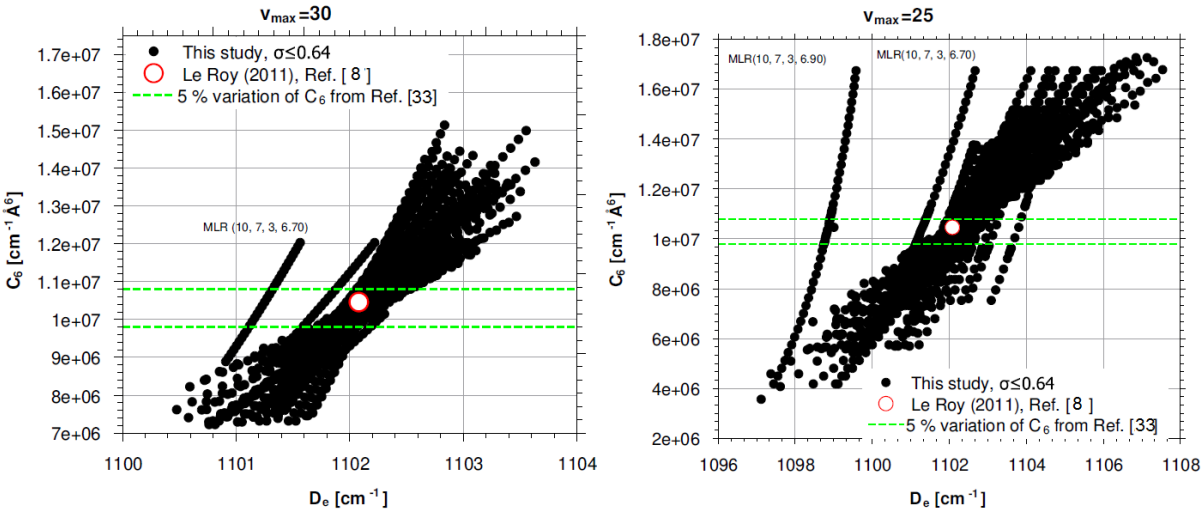

Figure 5. 4: Distribution of C_6 and D_e for MLR potentials (with $\sigma \leq 0.64$) fitted up to $v"_{max} = 30$ (left pane) and $v"_{max} = 25$ (right pane) derived by fixing C_6 within a broad range of values and refitting all other parameters. The best value from Ref. [8] is also shown. Some series of MLR types are designated as MLR (N, p, q, r_{ref}).

With the more reduced data sets Figure 5. 4 ($\nu"_{max} = 25$ and $\nu"_{max} = 30$) the uncertainties of C_6 from the fit are even larger and we prefer to estimate them by varying C_6 as done for $\nu"_{max} = 35$.

For $\nu"_{max} = 30$ we constructed about 6200 PECs, 3500 of them with $\sigma \leq 0.64$, for $\nu"_{max} = 25$ the number of fitted curves was 7800, about 5000 of them with $\sigma \leq 0.64$. The variation of C_6 was stopped when it significantly exceeded its initial value (by about 80 %) although for some potentials $\sigma \leq 0.64$ still could be reached. Apparently for the present data sets the value of C_6 may be virtually arbitrary. Here we should mention that the turning points of $\nu" = 25$ is about 7.6 Å and for $\nu" = 30$ – about 9.0Å , and both values are smaller than the Le Roy radius for the Ca_2 ground state (about 9.4 Å), so it is not surprising that the uncertainty of C_6 is so large. The estimate of D_e, however, is very reasonable and is within about $\pm 1.5 cm^{-1}$ for $\nu"_{max} = 30$ and $\pm 5\ cm^{-1}$ for $\nu"_{max} = 25$, and we believe this is the main result of present study.

By using a reasonably wide range of MLR parameters N, p, q and r_{ref} and also by varying C_6 much beyond the expected theoretical estimate, all "good" potentials ($\sigma \leq 0.64$) predict a pretty consistent value for D_e, which is also very close to the best-known experimental result. If the variation of C_6 is limited to within the expected few percent of the theoretical estimate, the uncertainty in D_e could be significantly reduced. Some series of MLR potentials have D_e and C_6, which obviously deviate from the main distribution. Both for $\nu"_{max} = 25$ and $\nu"_{max} = 30$ these are the types MLR ($N = 10, p = 7, q = 3,\ r_{ref} = 6.70$) and MLR ($N = 10, p = 7, q = 3,\ r_{ref} = 6.90$) (indicated in Figure 5. 4). The larger r_{ref} the slower y(r) tends to 1 as r increases, so the correlation with C_6 is stronger. Given $R_e \approx 4.3$ Å and the outermost turning point for $\nu"_{max} = 25$ about 7.6 Å makes the choice $r_{ref} = 6.7$ Å or even 6.9 Å unrealistic, though possible. Therefore, in practice one could ignore potential types with such large r_{ref}.

Chapter 6 Conclusions

The extrapolation properties of the analytic potentials had been addressed almost immediately after they were applied to data approaching the dissociation range. The initial results using simpler potential forms were not as good, because when the functions become flexible enough to fit the experimental data, the extrapolation becomes also unreliable.

We agree with Ref. [8] that the MLR potential may be a reasonable compromise when experimental data approach the dissociation limit. Some successful applications and the current study already confirm this, but only the experience collected in many different studies will enable the researchers to form a final opinion.

The numerical experiments presented in this paper aim to assess the extrapolation properties of the MLR potential form in a more general way, compared to [12] and [8]. The only criterium for the quality of the potential curve is the agreement with the available set of experimental data. The MLR potentials can be divided into classes with different values of $r_{ref}\ , p, q\ and\ N$. We did not study all possible combinations of these parameters, but set some reasonable limits, discussed already in [12] and [8]. The value for r_{ref} should be close to the equilibrium distance, p and q should be some small integers and $p\ +\ 6$ should be no smaller than 10 (6 being the power of the leading dispersion coefficient C_6, 10 – the power of the last coefficient, C_{10}). The number of β terms was kept small, just about the necessary number needed to achieve a good fit. With only these limitations we observed that the MLR form converges very close to the best estimate for the dissociation energy, even when extrapolating from relatively low v'' experimental data (the binding energy for $v'' = 25$ is approximately $1010\ cm^{-1}$, the energy for $v'' = 30$ is $1070\ cm^{-1}$). This result is unexpected because such long extrapolation is usually very unsafe. It indicates that the MLR potential may be a reliable model, which can achieve both experimental accuracy and good extrapolation accuracy, which is a very useful property when the experimental data does not reach the dissociation limit.

The C_6 coefficient itself cannot be determined as reliably as D_e from limited datasets, but it would be unreasonable to expect sensible values for the long-range parameters C_n, when the outermost turning points of the experimental data are well below the Le Roy radius, where the potential significantly deviates from the pure long-range form so change in C_n can be compensated by the short-range parameters β_i. The extrapolation properties of the MLR potentials may be further improved by using additional limitations of the possible values of C_n. This was also discussed in detail in the original MLR papers [12] and [8]. For example, the theoretical calculations in many cases set already quite tight uncertainty intervals around the calculated dispersion coefficients. In the present case of Ca_2, allowing for a 5% uncertainty in the theoretical C_6 will automatically reduce the uncertainty in D_e from $\pm\ 2\ cm^{-1}$ to about $\pm\ 1\ cm^{-1}$ for $v"_{max} = 30$.

The uncertainty intervals for D_e and C_6 determined from Figure 5. 2 and Figure 5. 1 are derived under specific choice of limiting values of σ. We are not claiming that this is the ultimate uncertainty associated with these long-range parameters of the Ca_2 ground state. Our aim is to show that within a large subset of MLR potential it is possible to have a consistent prediction for the dissociation energy of the electronic state. In combination with good theoretical value for C_6 the MLR form offers a reasonable long-range behavior of the electronic state even when the experimental data are well below the dissociation limit. For relatively full data sets, other potential models also can perform well, but none of them, to our best knowledge, has such good extrapolation properties. This conclusion comes from analyses of a single electronic state. To be more convincing, it should be supported with similar studies of various types of electronic states.

For further improvement on the Ca_2 ground state PEC, especially at long internuclear distances we believe that should be used only high-resolution Doppler free spectroscopic techniques.

Chapter 7 Contributions

Scientific contributions:

- For the first time the extrapolation properties of the Morse/Long Range potential have been investigated. It was shown that very reasonable values for D_e may be obtained even when the last 10-12 energy levels are missing.
- The leading coefficient C_6 cannot be fixed as reliably as D_e. At large extrapolations it is reasonable to use the theoretical values for C_6. Even a 5% uncertainty in C_6 may reduce significantly the uncertainty in D_e.
- A methodology is suggested for assessment of the uncertainties of the fitted parameters, due to the model dependences. Contrary to the uncertainties due to the errors of the experimental data, a systematic study of the model dependences is missing (to our best knowledge). Of course, the presented studies and considerations should by no means be treated as final, apparently a lot still needs to be done.

The author's personal contributions may be summarized as follows:

- Critical review of existing functional forms, suitable for modeling high resolution experimental data in diatomic molecules. Selection of functions with promising extrapolation at large internuclear distances – these are the Morse-Long-Range and the Chebishev-Polynomial-Expansion. Only the MLR form was studied extensively within the thesis.
- Active participation in building of the methodology of the study. The procedure presented in the thesis is only the final stage of the performed investigations. Many ideas have been tested which consumed hundreds of hours of computing time.
- Testing the newly written Fortran code **IPA8** in the part dedicated to the MLR function. Derivation of the derivatives of the function with respect to the parameters.
- All the work for preparation of the potentials before the automatized fitting: preparation of the initial potentials with the **betafit** program, fitting them with the **IPA8** code.
- Active participation in preparation of the simulations, collection of data, analysis of the results.

Full length paper:

1. A. Sinanaj and A. Pashov, Extrapolation properties of the Morse-Long Range potential at large internuclear Distances, J. Mol. Spectrosc. **396**, 111811 (2023).
2. A. Sinanaj and A. Pashov, Extrapolation properties of the Chebyshev-Polynomial-Expansion potential, Acta Physica Polonica A **146** (2024) in print

Conference papers:

2. A. Sinanaj and A. Pashov, Extrapolation Properties of the Morse/Long-Range Potential *Proceedings of Science, vol. 427 - 11th International Conference of the Balkan Physical Union (BPU11)* 2023.

Participation in conferences with posters:

1. 1-st International Scientific Conference in Mathematics and Physics, and their applications (1-st ISCMPA), 03 – 04 November 2022), Albania
2. The 11th Conference of the Balkan Physical Union (BPU11Congress), from 28 August to 1 September 2022.) Serbia, Poster presentation
3. 28th colloquium on High resolution molecular spectroscopy, 28 Aug to 1 Sept, 2023 Dijon, France

References

[1] O. Klein, « Zur Berechnung von Potentialkurven für zweiatomige Moleküle mit Hilfe von Spektraltermen », Vols. vol. 76, nos 3-4, Zeitschrift für Physik, (DOI 10.1007/BF01341814), 1932, pp. 226-235.

[2] R. Rydberg, « Über einige Potentialkurven des Quecksilberhydrids », Zeitschrift für Physik,, Vols. vol. 80, nos 7-8, Zeitschrift für Physik, (DOI 10.1007/BF02057312.), 1933, pp. 514-524.

[3] J. Hinze and W. Kosman, "Inverse Perturbation Analysis: Improving the Accuracy of the Potential Energy Curves.," *J. Mol. Spectrosc,* vol. 56, pp. 93-103, 1975.

[4] H. Scheingraber and C. R. Vidal, "Determination of Diatomic Molecular Constants Using An Inverted Perturbation Approach. J. Mol. Spectrosc.," *J. Mol. Spectrosc,* vol. 65, pp. 46-64, 1977.

[5] M. R. Doery, E. J. D. Vredenbregt, J. G. C. Tempelaars, H. C. W. Beijerinck and B. J. Verhaar, "Long-range diatomic s+p potentials of heavy rare gases," *Phys. Rev. A 57, 3603 – Published 1 May 1998,* vol. 57, no. 5, p. 3603, 1998.

[6] K. M. Jones, E. Tiesinga, P. D. Lett and P. S. Julienne, "Ultracold photoassociation spectroscopy: Long-range molecules and atomic scattering," *Rev Mod Phys,* vol. 78, no. 2, p. 483, 2006.

[7] R. J. Le Roy and R. B. Bernstein, "Dissociation Energy and Long-Range Potential of Diatomic Molecules from Vibrational Spacings of Higher Levels," *J Chem Phys,* vol. 52, no. 8, pp. 3869-3879, 1970.

[8] R. J. Le Roy, "Chapter 6 of Equilibrium Structures of Molecules.," in *Equilibrium Molecular Structures*, London, ed. J. Demaison and A. G. Csaszar. Taylor and Francis, 2011, pp. 159-203.

[9] O. Allard, A. Pashov, H. Knöckel and E. Tiemann, "Experimental study of the Ca2 1S+1S asymptote," *Phys. Rev. A,* vol. 66, p. 042503, 2002.

[10] O. Allard, C. Samuelis, A. Pashov, H. Knöckel and E. Tiemann, "Experimental study of the Ca2 1S+1S asymptote.," *Eur. Phys. J. D.,* vol. 26, pp. 155-164, 2003.

[11] R. Moszynski, G. Lach, M. Jaszunski and B. B. Honvault, "Long-range relativistic interactions in the Cowan-Griffin approximation and their QED retardation: Application to helium, calcium, and cadmium dimers," *Phys. Rev. A,* vol. 68, p. 052706, 2003.

[12] R. J. Le Roy and R. D. E. Henderson, "A new potential function form incorporating extended long-range behaviour: application to ground-state Ca2," *J. Mol Physics,* vol. 105, pp. 663-677, 2007.

[13] E. Pachomov, V. P. Dahlke, E. Tiemann, F. Riehle and U. Sterr, "Ground-state properties of Ca_2 from narrow-line two-color photoassociation.," *Phys. Rev. A,* vol. 95, p. 043422, 2017.

[14] M. Lepers and O. Dulieu, "Long-range interactions between ultracold atoms and molecules.," *Physical Chemistry. Chem. Physic,* no. arXiv:1703.02833v2 [quant-ph], 9 Apr 2017.

[15] R. J. Le Roy, Molecular Spectroscopy, In: Barrow RN, Long DA, Millen DJ, editors. Specialist periodical report 3,, Vols. Vol 1,, D. A. L. a. D. J. M. Eds. R. F. Barrow, Ed., London: Chemical Society of London;, 1973, pp. 76-113.

[16] M. Marinescu and H. R. Sadeghpour, "Long-range potentials for two-species alkali-metal atoms.," *Phys. Rev. A,* vol. 59, pp. 390-404, 1999.

[17] A. Dalgarno and M. Marinescu, "Dispersion forces and long-range electronic transition dipole moments of alkali-metal dimer excited states.," *Phys. Rev. A,* vol. 52, pp. 311-328, 1995.

[18] M. Marinescu and A. F. Starace, "Dispersion coefficients for highly exited molecular states of K_2.," *Phys. Rev. A,* vol. 56, pp. 4321-4323, 1997.

[19] M. Marinescu, "Dispersion coefficients for the nP-nP asymptote of homonuclear alkali-metal dimmers.," *Phys. Rev. A,* vol. 56, pp. 4764-4773, 1997.

[20] S. Porsev and A. Derevianko, "High-accuracy relativistic many-body calculations of van der Waals coefficients C6 for alkaline-earth-metal atoms," *Phys. Rev. A,* vol. 65, p. 020701, 2002 S..

[21] M. Tamanis, R. Ferber, A. Zaitsevskii, E. A. Pazyuk, A. V. Stolyarov, H. Chen, J. Qi, H. Wang and W. C. Stwalley, "High resolution spectroscopy and channel-coupling treatment of NaBr," *J. Chem. Phys,* vol. 117, no. 17, pp. 7980-7988, 2002.

[22] I. Havalyova, A. Pashov, P. Kowalczyk, J. Szczepkowski and W. Jastrzebski, "The coupled system in Rb_2," *JOURNAL OF QUANTITATIVE SPECTROSCOPY & RADIATIVE TRANSFER,* vol. 202, pp. 328-334, 2017.

[23] A. Pashov, P. Kowalczyk, A. Grochola, J. Szczepkowski and W. Jastrzebski, "Coupled-channels analysis of electronic states in rubidium dimer," *JOURNAL OF QUANTITATIVE SPECTROSCOPY & RADIATIVE TRANSFER,* vol. 221, pp. 225-232, 2018.

[24] J. Szczepkowski, A. Grochola, P. Kowalczyk, W. Jastrzebski, E. A. Pazyuk, A. V. Stolyarov and A. Pashov, "The spin-orbit coupling in KCs: Observation and deperturbation.," *Journal of Quantitative Spectroscopy and Radiative Transfer,* vol. 239, p. 106650, 2019.

[25] P. Jasik, P. Łobacz and J. E. Sienkiewicz, "Potential energy curves, transition and permanent dipole moments of KRb,," *Atomic Data and Nuclear Data Tables.,* vol. 149, p. 101558, 2023.

[26] U. Kleinekathofer, K. T. Tang, J. P. Toennies and C. L. Yiu, "Angular momentum coupling in the exchange energy of multielectron systems.," *J. Chem. Phys.,* vol. 103, pp. 6617-6630, 1995.

[27] W. H. Press, S. A. Teukolski, W. T. Vetterling and B. P. Flannery, Numerical Recipes in Fortran 77., New York, USA: Cambridge University Press, 1992.

[28] R. J. Le Roy and A. Pashov, "dPotFit: A computer program to fit diatomic molecule spectral data to potential energy functions," *J. Quant. Spectrosc. Rad. Trans,* vol. 186, pp. 210-220, 2017.

[29] J. Y. Seto, R. J. Le Roy, J. Vergès and C. Amiot, "Direct potential fit analysis of the X^1 Σ_g^+ state of Rb2. Nothing else will do!," *J. Chem. Phys.,* vol. 113, pp. 3067-3076, 2000.